Endothelial cells as mechanical transducers: Enzymatic activity and network formation under cyclic strain

A. Shukla[1], A.R. Dunn[2], M.A. Moses[3] and K.J. Van Vliet[4]

Abstract: Although it is established that endothelial cells can respond to external mechanical cues (e.g., alignment in the direction of fluid shear stress), the extent to which mechanical stress and strain applied via the endothelial cell substrate impact biomolecular and cellular processes is not well-understood. This issue is particularly important in the context of inflammation, vascular remodeling, and cancer progression, as each of these processes occurs concurrently with localized increases in strain and marked changes in molecules secreted by adjacent cells. Here, we systematically vary the level and duration of cyclic tensile strain applied to human dermal microvascular and bovine capillary endothelial cells via substrate deflection, and then correlate these cues with the secretion of extracellular matrix-degrading enzymes and a morphological transition from confluent monolayers to well-defined multicellular networks that resemble capillary tube-like structures. For a constant chemical environment, we find that super-physiological mechanical strain stimulates both endothelial cell secretion of latent matrix metalloprotease-2 and multicellular networks in a time- and strain-dependent manner. These results demonstrate coupling between the mechanical and biochemical states of microvascular endothelial cells, and indicate that elevated local stress may directly impact new capillary growth (angiogenesis) toward growing tumors and at capillary wall defect sites.

keyword: endothelial cells, MMP-2, proteolysis, strain, mechanotransduction, angiogenesis

1 Introduction

Vascular endothelial cells (ECs) represent the primary cell type comprising new vessels during normal or pathological vascular remodeling. Angiogenesis, the sprouting of new capillaries from pre-existing vasculature, is a critical process involved in vascular remodeling that is desirable after cardiac trauma such as heart failure and undesirable in the presence of tumors that transition from the benign to malignant state upon sufficient vascularization, the so-called "angiogenic switch," as well as the maintenance and growth of a malignant tumor [Hanahan and Folkman (1996)]. Although the chemical cues by which angiogenesis can be promoted and suppressed are well-studied and increasingly well-understood, the mechanical cues which may impact vascular remodeling have not been addressed systematically. As the concepts and approaches herein draw from fields with distinct histories and vocabularies, we first summarize the current state of knowledge regarding endothelial cell mechanotransduction; a proteolytic enzyme key to vascular and extracellular matrix remodeling; and the coupling between mechanical state and the secretion of this enzyme in other cell types.

1.1 Endothelial cell chemomechanical coupling

The shape, cytoskeletal structure, and function of individual, vascular ECs are affected strongly by mechanical cues imposed by fluid shear flow, as in the physiological state of pulsatile fluid flow through EC-lined vasculature [Davies *et al.* (1995); Davies *et al.* (1997); Drenckhahn and Ness (1997); Hsiai *et al.* (2002); Lee *et al.* (2002); Shyy and Chien (2002); Resnick *et al.* (2003)]. Although the mechanisms by which ECs transduce shear deformation into biochemical signals and cytoskeletal reorganization are not fully clear [Ingber (2002); Liu *et al.* (2002); Shyy and Chien (2002)], it is generally accepted

---

[1] The Center for Materials Science and Engineering and the Materials Processing Center Research Experience for Undergraduates, MIT, Cambridge, MA, and Departments of Chemical and Biomedical Engineering, Carnegie Mellon University, Pittsburgh, PA, U.S.A.

[2] Department of Biology, Colorado College, Denver, CO, U.S.A.

[3] Vascular Biology Program, Children's Hospital, and Department of Surgery, Harvard Medical School, Boston, MA, U.S.A.

[4] Vascular Biology Program, Children's Hospital, Boston, MA, U.S.A. and Department of Materials Science & Engineering, MIT, Cambridge, MA, U.S.A

that confluent monolayers of ECs align in the direction of shear flow and that the extracellular matrix adjacent to the ECs significantly attenuates the velocity of fluid flow adjacent to the cell membrane [Weinbaum *et al.* (2003)].

Further, it is established that population-level morphological changes from EC monolayers to networks comprising capillary tube-like structures can be promoted through biochemical stimuli. This marked change is termed morphological differentiation, as ECs transition from a proliferative to a nonproliferative state during this reorganization that is required for formation of functional capillaries and venules [Kubota *et al.* (1988)]. For example, capillary tube formation occurs on the timescale of several days to several weeks for various EC types under two-dimensional (2D) *in vitro* culture conditions, e.g., on gelatin-coated polystyrene in the absence of soluble proteins such as endothelial cell growth factor, ECGF [Folkman and Haudenschild (1980)]. In contrast, this morphological differentiation occurs in less than 24 hrs for the same types of ECs cultured *in vitro* on gels rich in certain ECM proteins. Tube formation assays, increasingly common *in vitro* tests of biochemical control of angiogenesis, are conducted using commercially available basement membrane analogues, such as Matrigel® (Becton Dickinson) comprising laminin (60%) and gelatin (30%), have established that the presence of these extracellular matrix-bound proteins stimulates formation of networks comprising capillary tube-like structures of 10 μm diameter within the three-dimensional (3D) gel, and that these 3D cylinders comprise anastamosing (fusing) cells with patent lumens [Kubota *et al.* (1988)]. Thus, biochemical cues can induce tube formation, and mechanical cues can induce cellular polarization.

1.2   Matrix metalloprotease-2 and angiogenesis

Matrix metalloproteases (MMPs) are members of a family of metal-dependent ectoenzymes. Historically, these enzymes are numbered in order of discovery and grouped into five categories based on substrate specificity. For example, MMP-2 and MMP-9 are gelatinases, indicating primary specificity for and proteolytic degradation of gelatin, or collagen IV. Both of these gelatinases contain three cysteine-rich repeats within the catalytic domain of the molecule; these regions bind and cleave gelatin [Sternlicht and Bergers (2000)]. The presence of MMP-2 increases significantly in pathologies such as rheumatoid arthritis and malignancies such as cancer (Stern-

licht and Bergers, 2000). Further, it is known that tumor cells express proteases including MMP-2 *in vitro* and *in vivo* [Apodaca *et al.* (1990); Nakano *et al.* (1995)]. Like all ectoenzymes in this family, MMP-2 contains a structural domain termed the "pro-domain" that maintains the latency or inactivity of the enzyme until it is removed or disrupted; the inactive form is termed latent or proMMP-2 [Nagase and Woessner (1999)]. The presence of this pro-domain provides a means of control over MMP-2 activity [Strongin *et al.* (1995); Lohi *et al.* (2000)], as this enzyme is constitutively expressed by most cells including vascular and capillary ECs. Although the mechanisms by which secreted MMP-2 is activated have not been established conclusively, it is generally accepted that MMP-2 activation requires formation of a dynamic complex among a tissue inhibitor of metalloproteases, TIMP-2, a membrane-bound MMP, MT1-MMP, and MMP-2 [Strongin *et al.* (1995)].

In the simplest description of angiogenesis, new capillaries sprout from existing capillaries via the local degradation of the protein-based basement membrane and extracellular matrix (ECM) surrounding existing capillaries. This process is mediated by the activation of secreted and cell membrane-bound MMPs [Moses (1997); Fang *et al.* (2000)]. Although the biochemical activation of MMPs is well-studied, activation via mechanical strain is relatively unexplored. It is plausible that elevated mechanical stress (due to defects in vessel walls, cyclic vessel wall stress during pulsatile blood flow, or compressive and tensile stresses from growing tumors) impacts enzymatic responses and the subsequent angiogenic response of vascular endothelial cells. This hypothesis can be tested by monitoring the expression and activity of MMPs and the morphological response of endothelial cell populations as a function of controlled mechanical environments.

1.3   Mechanical stimulation of MMP-2 in other cell types

It is known qualitatively that the expression of MMPs as a general class of enzymes can be regulated by environmental cues including cell stress [Kheradmand *et al.* (1998)]. Several researchers have recently explored quantification of mechanical stress and metalloprotease response in the context of cell types which are known to impose and respond to mechanical cues. Such cells include fibroblasts that impose substrata contraction and

other tissue remodeling processes during wound healing. Prajapati *et al.* monitored the fibroblast-mediated contraction of three-dimensional collagen-based scaffolds under conditions of zero applied load, constant applied load and stress relaxation, and correlated the extent of scaffold contraction with the secretion of latent and active metalloproteases by these fibroblasts using gel electrophoresis and zymography. These authors found that secretion of both MMP-2 and MMP-9 increased with increasing applied strain, due presumably to increased, opposing contraction by fibroblasts. Further, in this cell type and under these mechanical conditions, nearly 100% of MMP-2 was secreted in the latent form, whereas up to 80% of MMP-9 was secreted in the active form [Prajapati *et al.* (2000a)]. A separate study by the same authors quantified the characteristics of external load-controlled deformation to which fibroblasts were most responsive: ramp loading to 1.20 mN at loading rates ranging from 0.03 - 2 μN/s, and cyclic loading variations to the same maximum load at a rate of 0.7 μN/s for 16 cycles at a cyclic frequency of 0.5 Hz. The authors found that MMP-2 was up-regulated under ramp loading, but not under cyclic loading; active MMP-9 was up-regulated under both loading regimes [Prajapati *et al.* (2000b)].

Here, we correlate the application of cyclic strain with the secretion of MMP-2 and the local reorganization of confluent endothelial cells under two-dimensional *in vitro* conditions. By investigating how external mechanical deformation directs ECM-degradation and subsequent cell organization, we may better understand how developmental and pathological processes depend on mechanical stimuli.

2   Methods

2.1   Cell culture

We obtained primary, bovine capillary endothelial cells (CECs) through the generosity of C. Butterfield and Dr. J. Folkman (Vascular Biology Program, Children's Hospital Boston) and maintained these cells in full media comprising Dulbecco's Modified Eagle's Medium (DMEM, JRH Biosciences) supplemented with 10% calf serum (HyClone), 1% glutamine penicillin streptomycin (Irvine Scientific), and 3 ng/mL basic fibroblast growth factor (bFGF, Scios Nova) at 37°C and 10% CO_2. We obtained a commercial line of human dermal microvascular endothelial cells (HMVECs, Cambrex), and main-

tained these cells in endothelial basal media-2 supplemented with co-packaged fetal bovine serum, antibiotics and growth factors (Clonetics) at 37°C and 5% CO_2. Cells were supplied with fresh, full media every other day and passaged weekly.

2.2   Cyclic substrate deformation experiments

We imposed cyclic deformation on confluent monolayers of each cell type via a commercial servo-controlled system (FX-4000T Flexercell® Tension Plus, Flexcell Int.), a bioreactor capable of imposing near-physiological strain conditions. This system employs vacuum pressure to deflect the collagen type I-coated, silicone substrate (35 mm diameter, 0.5 mm thickness) within a polystyrene 6-well plate (BioFlex®, Flexcell Int.) in which cells are cultured. Prior to cyclic loading, we aspirated serum-containing media (full media) from all wells, rinsed wells thoroughly with 150 mM phosphate-buffered saline (PBS), and replaced with 2 mL of serum-free media in order to eliminate the background of enzymes present in serum. Control plates were maintained in parallel, including media exchange immediately prior to cycling of the test plates, and incubation adjacent to the test plates for the appropriate duration of cyclic strain experiments. We confirmed that neither apoptosis nor MMP-2 levels were affected over up to 12 and 24 hours in HMVECs and CECs, respectively, and that the presence of as little as 1% serum included enzyme levels significantly greater than the serum-free response (data not shown). We then loaded wells cultured to at least 75% confluence into a rubber-gasketed plate that facilitated vacuum aspiration within a standard water-jacketed incubator (37°C), and applied fixed levels of maximum strain amplitude at a cyclic frequency of 0.5 Hz consistent with physiological frequency. Control plates were positioned alongside, rather than inside, the gasketed plate. At the conclusion of each cyclic loading experiment, supernatant was collected from each well, aliquotted and immediately stored at -20°C.

We intentially chose to investigate strain amplitudes that reflected super-physiological levels of stress, as follows. Substrate displacement h can be measured as a function of applied vacuum aspiration pressure P and expressed as nominal applied strain amplitude ε as shown in Fig. 1a (reported by the manufacturer and confirmed in our experiments). This relationship is nonlinear elastic, in that there is essentially no deformation hysteresis over a com-
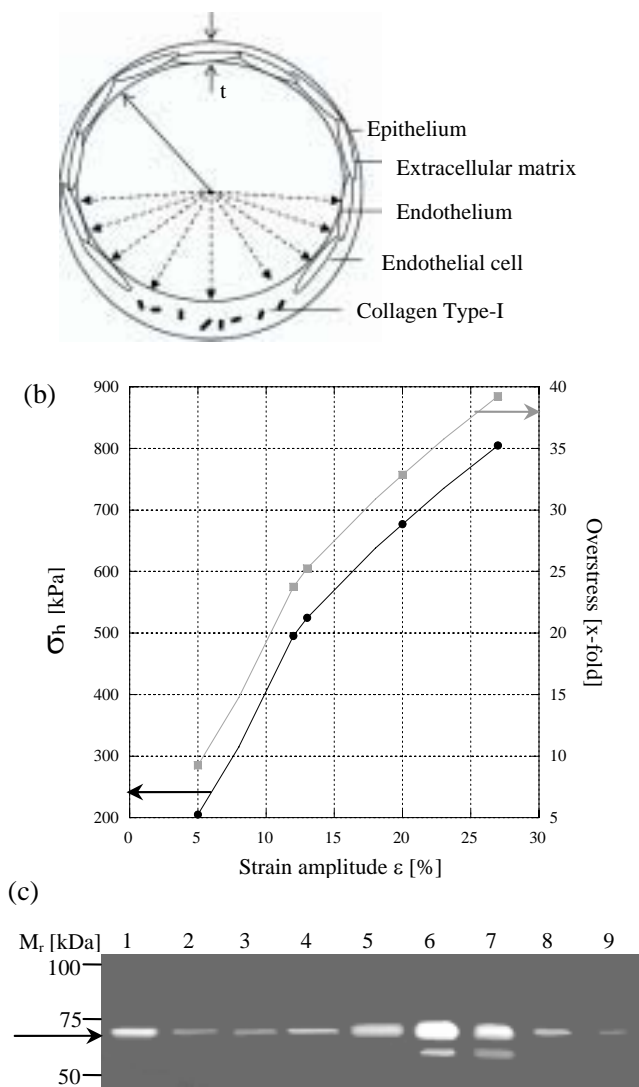
Figure 1 : Experimental design. (a) Schematic of capillary wall stress determinants. (b) Calculated relationship between hoop stress $\sigma_h = Pr/t$ as a function of substrate strain amplitude ε (left axis) and extent to which experimentally imposed values of σ_h exceed basal levels of stress in capillaries (right axis). Variables defined in Tab. 1. (c) Gelatin zymogram indicating presence of 72 kDa proMMP-2 (arrow) in HMVEC supernatant. Lane description: 1: ε= 0.0 , 4 hrs; 2: ε = 0.8, 4 hrs; 3: ε = 0.12, 4 hrs; 4: ε = 0.18, 4 hrs; 5: ε = 0.23,4 hrs; 6: 4.50 ng proMMP-2; 7: 1.50 ng proMMP-2; 8: 0.50 ng proMMP-2; 9: 0.25 ng proMMP-2.

plete loading-unloading cycle. For silicone wells of this diameter and well height, the maximum strain that can be attained in this system is approximately 0.30, beyond which the silicone substrate contacts the rubber-gasketed plate. To relate the stress resulting from this substrate deformation to basal levels of physiological stress, we express the effective radius of the deflected substrate r as

$$r = (c^2 + 4h^2)/(8h) \tag{1}$$

where c is cord half-width of an effective sphere of radius r, and express the effective circumferential or hoop stress σ_h as

$$\sigma_h = Pr/t \tag{2}$$

where t is substrate thickness. Physiological and experimental values of P, r, and t are shown in Tab. 1. Within a capillary, P represents internal pressure due to fluid flow, and r and t represent capillary radius and wall thickness, as shown in Fig. 1a. The resulting maximum hoop stress within a capillary under normal physiological conditions (basal σ_h) is approximately 20 kPa. As the silicone substrate thickness used in the present experiments significantly exceeds capillary wall thickness, we identified the product of aspiration pressure and effective radius Pr such that the stress applied to cells on silicone would be equivalent (approximately 10 N/m). In fact, physiological, basal hoop stress would require applied nominal strain of $< 1\%$ in the present experimental system. As the purpose of these experiments was to consider super-physiological strain amplitudes concurrent with local stress concentrations, we chose strain amplitudes resulting in overstresses as indicated in Fig. 1a, up to 800 kPa or a 40-fold excess of maximum, basal levels of capillary hoop stress. For CEC studies, we applied strain amplitudes ε of 0.0, 0.13, 0.20 and 0.27 over 24 hrs or total number of cycles N = 42,200; for HMVEC studies we applied ε of 0.0, 0.08, 0.12, 0.18 or 0.23 over both 4 hrs (N = 7,200) and 12 hrs (N = 21,600). Note that the above 4 hr and 12 hr time points were separate experiments, not continuations of a single experiment for a given cell population. Thus, the stress levels explored experimentally correlate with stress concentrations and externally applied stresses significantly exceeding those due to flow within the capillary, and are consistent with potential stress concentrations resulting from capillary wall defects and branch points, as well as recently re-

Table 1 : Experimental and physiological variables[5]

	r [mm]		t [mm]	P [kPa]	σ [kPa]	
	Min	Max			Min	Max
Capillary	0.0020	0.0045	0.0005	2.26	9	20
Experiment	18	32	0.5	0-21.60	205	805

ported tensile strains of up to 0.30 exerted by growing tumors *in vitro* [Gordon *et al.* (2003)].

2.3 Zymography

We determined the presence of MMP-2 through gelatin zymography, an established molecular biology ectoenzyme assay that relies on the ability of MMP-2 to degrade gelatin that is copolymerized within a sodium dodecyl sulfate-polyacrylamide gel upon electrophoresis (SDS-PAGE). Note that the latent enzyme is still detectable in this assay due to the conformational changes in MMPs subject to SDS-gelatin-copolymerized-PAGE; Molecular weight distinguishes this latent form (72 kDa) from the active form (68 kDa).

We collected serum-free supernatant from the HMVEC silicone wells, after either 4 hours or 12 hours of cyclic mechanical strain (ε = 0.0, 0.08, 0.12, 0.18, and 0.23), and normalized sample volume by cell number as measured through a particle counter (BeckmanCoulter). In order to ensure a detectable latent MMP-2 signal, we concentrated each sample tenfold via microcentrifugation (Denville 260D) in filtered vials (Nanosep 3K Omega) at 4°C. We obtained constant sample volume of 20 μL/lane via supplementation with serum-free media of appropriate type and buffered each sample with 10 μL of 0.5 M Tris, 50% glycerol, 10% SDS, and Bromophenol Blue. To determine molecular weight over the range of 10 to 250 kDa, we included a standard commercial marker (Precision Plus, Bio-Rad Laboratories). To quantify the amount of MMP-2 present in each lane, we included a serial dilution of commercially pure proMMP-2 (Calbiochem) in 50 mM Tris Base, 5 mM CaCl$_2$, pH 7.5.

We subjected each 10%-gelatin polyacrylamide gel (In-

vitrogen) to electrophoresis (XCell SureLock Mini-Cell, Invitrogen) in a 3 Tris: 14.4 glycine: 1 SDS running buffer at 150 V for 125 min. Upon conclusion of electrophoresis, we removed SDS through rinsing (2 x 20 min) in 2.5% Triton X-100 (Sigma), and then rinsing in a buffer containing salts optimized for gelatinase activity (50 mM Tris-HCl, 200 mM NaCl, 5 mM CaCl$_2$, 0.02% Brij-35, pH 7.5, Bio-Rad Laboratories). We then incubated the gel in fresh gelatinase buffer overnight at 37°C under gentle agitation. After incubation, we removed the gelatinase buffer and stained the gel with 0.5% Coomassie staining buffer (20 min), followed by up to 80 min of destaining in 30% ethanol, 10% acetic acid. The location of gelatinase bands is observed as a distinct white color against the blue background of the Coomassie-stained gel, as shown in Fig. 1c. After destaining, we immediately scanned the gel to produce a digitized image of these clearance zones (CanoScan LiDE 30 Flatbed Scanner, Canon) and then archived the gel through drying in 10% glycerol-immersed cellophane.

Here, the enzyme type represented by the clearance zone was identified through co-analysis of pure proMMP-2 serial dilution within each gel, and confirmed by immunoblot analysis using a monospecific antibody (data not shown). We conducted densitometric analysis of the digitized gel image, specifically quantifying the density of bands corresponding to proMMP-2 (72 kDa). Using commercially available image processing software (Adobe Photoshop 7.0) and our customized analytical program, we computed the luminosity (average pixel luminosity for a given clearance zone) and size (number of pixels in a given clearance zone) to calculate the size-weighted or relative band luminosity (RBL) for each lane. By obtaining the relative band luminosities of the MMP-2 serial dilution, we calibrated the total mass of

---

[5] Capillary data taken from West, J.B., and Mathieu-Costello, O. (1995). Circulation 92, 622-631.

proMMP-2 as a function of RBL. Using this curve and relative band luminosity for each sample, we determined the amount of proMMP-2 corresponding to each 72 kDa band in units of ng/10,000 cells. In this manner, the amount of proMMP-2 present in each sample can be calculated consistently and can be compared within and among gels as a function of strain amplitude and total cycles. Each strain condition was analyzed in this manner in triplicate to determine experimental error as indicated by the error bars in Figs. 2 and 5.

2.4 Cell Image Analysis

We acquired digital photographs of the HMVECs immediately after 4 hrs and, in separate experiments, after 12 hrs of cyclic strain at each strain amplitude point. In the same manner, we acquired images of CECs taken before and after stretching for 24 hrs. For all images, we then parameterized the network in terms of diameter and area density (number/mm^2) through direct tracing of cell-free contours using commercially available image manipulation software (Adobe Photoshop 7.0). Three images per condition, representing the center region of each well, were analyzed and averaged.

3 Results

3.1 MMP-2 Activity

Below, we consider the effects of cyclic strain on the secretion of MMP-2 in both a human cell line and a primary bovine cell type. Note that active MMP-2, and active and latent MMP-9 were not observed for either cell type, either under typical *in vitro* conditions or under mechanical strain. This is consistent with other reports for similar EC types [Yan *et al.* (2000)]. Further, we did not observe differences in the levels of proMMP-2 secreted by either cell type as a function of substrate material (type IV collagen-coated polystyrene or type I collagen-coated silicone) for $\varepsilon = 0$.

3.1.1 Human dermal microvascular endothelial cells

The variation of proMMP-2 as a function of applied strain is shown in Fig. 2. Clearly, the amount of proMMP-2 secreted per HMVEC varies with applied strain. At early time points (t = 4 hrs) typical of mRNA expression analysis, proMMP-2 secretion decreases below basal levels for $\varepsilon = 0.08$, then cycles between basal and sub-basal levels until a sharp increase at $\varepsilon = 0.23$. In contrast, at later time points considered sufficient to evaluate changes in levels of functional proteins including MMPs (t = 12 hrs), peak secretion of proMMP-2 occurs at $\varepsilon = 0.12$, and decreases to a relatively constant value for greater strain amplitudes. However, the proMMP-2 level at a strain level of 0.23 is 26% greater than that measured under zero applied strain. Thus, it appears that although there is a positive correlation between applied strain and proMMP-2 secretion at t = 12 hrs, a peak response is observed at intermediate strain amplitudes. It is interesting to note that although one might expect MMP-2 levels to increase with elapsed time/elapsed cycles at all time points for $\varepsilon > 0$, we repeatedly observed a significant decrease in proMMP-2 secreted by HMVECs from 4 to 12 hours for $\varepsilon = 0.23$. This indicates that there is a strain limit beyond which proMMP-2 secretion is not stimulated under cyclic deformation.

As each experiment was conducted for a constant biochemical environment, a relatively constant cell number and a fixed cyclic frequency and number of mechanical cycles, it is reasonable to consider this variation in proMMP-2 by the HMVECs as a direct result of cyclic strain applied through the underlying substrate.

3.1.2 Bovine capillary endothelial cells

Figure 2 also indicates the secretion of proMMP-2 by CECs as a function of cyclic strain over 24 hrs. Similar to HMVECs at 12 hrs, there exists a peak level of proMMP-2 at an intermediate strain amplitude of $\varepsilon = 0.20$. Although we did not evaluate intermediate time points, the levels of proMMP-2 measured at 24 hrs for $\varepsilon = 0$ were consistently greater than that measured at any subsequent strain condition at 24 hrs.

3.2 EC Population Morphology

Here, we demonstrate for the first time the effects of cyclic mechanical strain on the formation of capillary tube-like network formation in 2D culture. Although we did not expect to observe dramatic morphological changes in the organization of confluent cell monolayers subjected to cyclic loading, the time- and strain-dependence of this observation in two distinct EC cell types under otherwise constant biochemical environment merits careful consideration. Figure 3 compares the morphology of CEC populations after 24 hrs at $\varepsilon = 0$ (Fig. 3a) and $\varepsilon = 0.27$ (Fig. 3b). Clearly, there is significant reorganization of the confluent monolayer into a
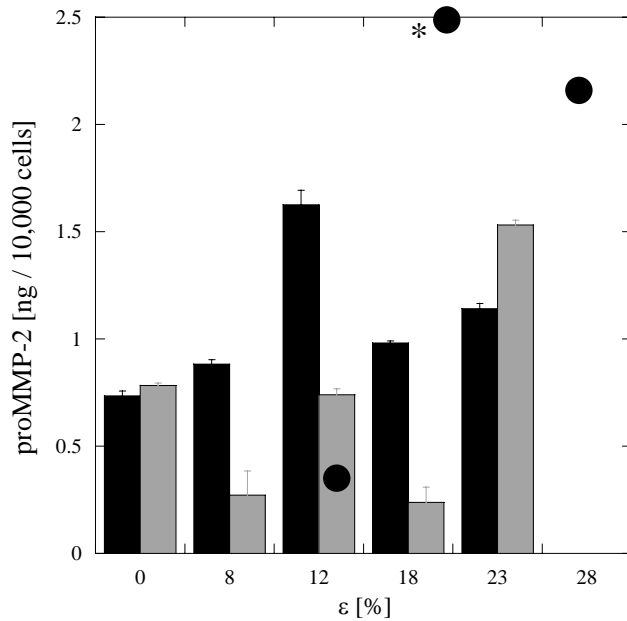
Figure 2 : Secreted proMMP-2 as a function of cyclic strain amplitude over 4hrs (gray) and 12 hrs (black) for HMVECs, and over 24 hrs (filled circles) for CECs (*circle: 4.40 ng/10,000 cells). Error bars indicate standard deviation for data analyzed in triplicate.

network of EC-dense struts. As we did not confirm that these structures actually exhibit patent lumens, we refer to these cell-dense regions comprising the networks as EC struts, but note that these structures closely resemble the early stages of capillary tube networks formed in response to biochemical stimuli and in the absence of controlled mechanical stimuli [Folkman and Haudenschild (1980); Kubota *et al.* (1988)]. It may be argued that these dramatic changes in organization are a 2D-analogue of tissue formation and remodeling observed in 3D biosystems. Below, we discuss these organizational changes in terms of the area density of and strut diameter within this network as a function of cell type, cyclic strain amplitude, and total cycles.

Figure 4 shows the density of this network as the number of annuli circumscribed by the EC-dense struts per mm^2 of substrate surface area ρ_R and the average annuli diameter defined by the inter-strut spacing d_R, as a function of strain at 4 hrs ($N = 7,200$) and 12 hrs ($N = 21,600$). At early time points and low number of elapsed cycles, ρ_R increases with increasing strain as the ECs aggregate, whereas d_R plateaus to relatively constant diameter of
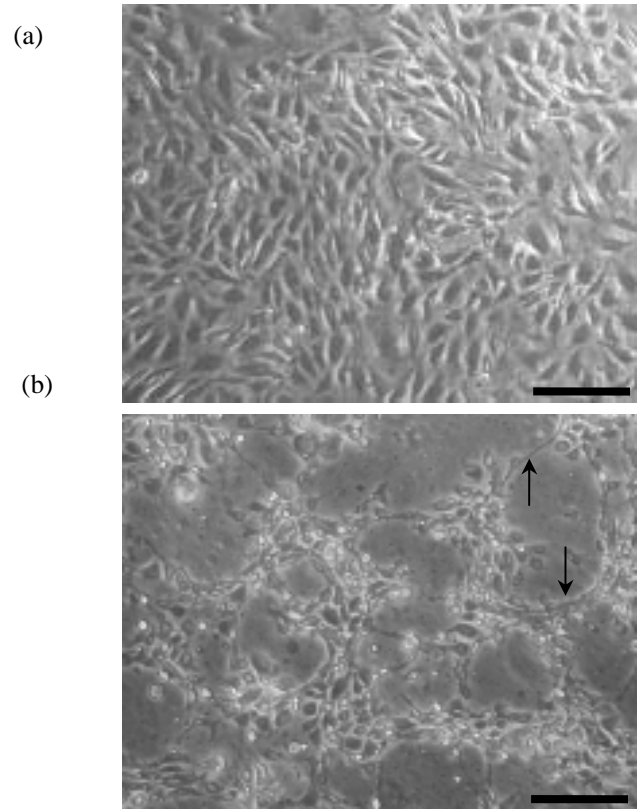

Figure 3 : Digitized optical images of CECs after 24 hrs for (a) $\varepsilon = 0.0$; (b) $\varepsilon = 0.27$. Note reorganization of (a) monolayer into (b) network of EC-dense struts [arrows] that circumscribe EC-free annuli. Note elongated and anastamosing cells along annuli perimeters. Scalebar = 65 μm.

250 μm at $\varepsilon = 0.12$. This indicates that the number of EC-dense struts (or tubes) formed is a stronger function of strain than the spacing of these struts, at least at early timepoints. After 12 hrs of cyclic strain, ρ_R increases with respect to the 4 hr timepoint for $\varepsilon < 0.23$, and saturates at ~ 4 annuli/mm^2. This indicates that the density of EC-dense struts appears to reach a maximal value that can be attained either by increasing strain amplitude or increasing number of cycles at a given strain amplitude $\varepsilon > 0.12$. In contrast, the spacing between these struts d_R increases modestly with ε for $\varepsilon < 0.23$, but increases markedly for $\varepsilon = 0.23$. Together, these results indicate that mechanical strain induces network formation such that the number and spacing of tube-like structures is dependent on the amplitude and duration of cyclic strain.
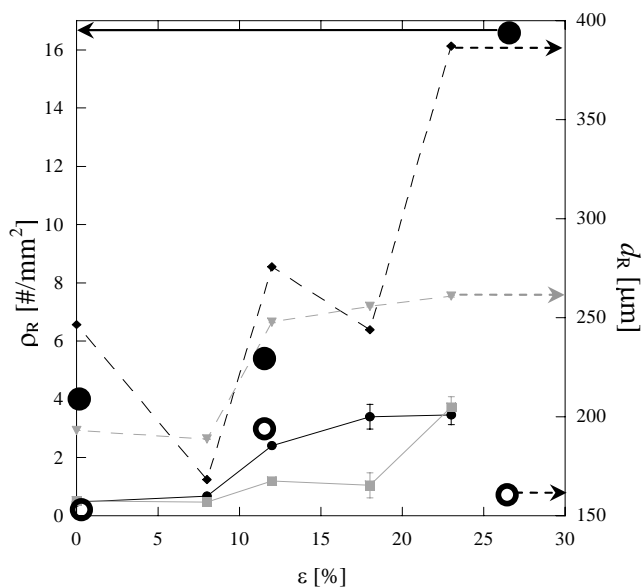
Figure 4 : Average network density *R*, as number of annuli per mm^2 of substrate area (solid line), and average diameter of these annuli d_R (dashed line) for HMVECs at ε = 0 - 0.23 after 4 hrs (gray) and 12 hrs (black), and for CECs after 24 hrs (ρ_R = open circles; d_R = closed circles). Error bars represent standard deviation of data analyzed in triplicate.

Note that this average spacing between EC-dense struts d_R (70 μm) significantly exceeds the diameter of the EC-dense struts ($\sim$20 μm). Further, under the maximal ε and N considered herein, ECs elongate but do not exhibit complete anastamosis as observed for t > 18 hrs in Matrigel® cultures (Kubota *et al.* (1988)).

Figure 4 also indicates the number and diameter of annuli observed over 24 hrs of cyclic strain in CECs. Here, note that the network density is greater than that observed for HMVECs. We did not observe that the average diameter of the struts within the network (capillary tube-like structures) was a function of time or strain in either cell type (data not shown). We did not observe network formation in HMVEC or CEC monolayers subjected to hypoxia or serum depletion/starvation over 12 hrs (data not shown), as consistent with findings for these and other EC types (Maciag *et al.*, 1982). In addition, we observed that total cell number at 12 hrs was not a function of applied strain amplitude, indicating that this network formation is the result of reorganization of the monolayer rather than the selective detachment of cells within the monolayer and
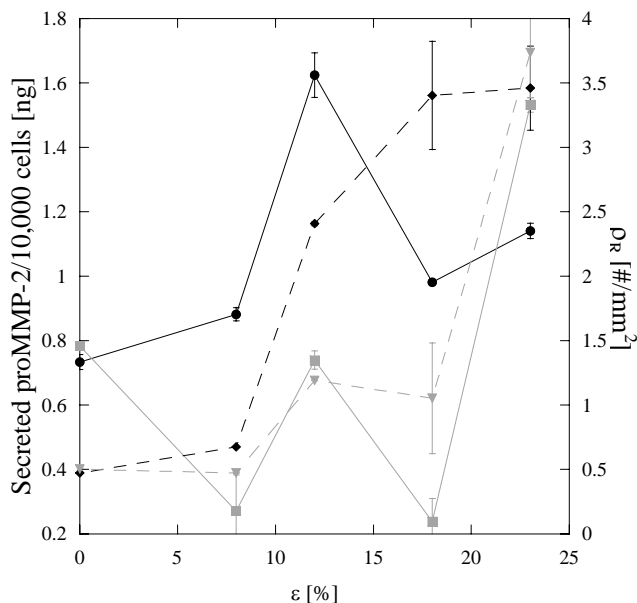

Figure 5 : Secreted proMMP-2 per 10,000 HMVECs (solid) and network density ρ_R (dashed) and at 0, 0.08, 0.12, 0.18, and 0.23 after 4 hrs (gray) and 12 hrs (black).

consistent with studies in gel-based capillary tube formation (Kubota *et al.*, 1988).

4 Discussion

Here, we interpret these trends in population-level reorganization of ECs as a mechanically induced change in the reserve levels of enzymes such as MMP-2 that facilitate degradation of the ECM during formation of capillary networks.

Figure 5 compares the levels of secreted proMMP-2 with the density of rings formed as a function of cyclic strain amplitude and duration for HMVECs at 4 hr and 12 hr time points (*N* = 7,200 and 21,600 cycles, respectively). This comparison demonstrates the coupling between the mechanical environment of these cells and the resulting changes in both enzymatic activity and population organization. Regression analysis of these data, as summarized in Tab. 2, provides empirical relationships which can be explored experimentally. We find that secretion of proMMP-2 is a nonlinear function of strain amplitude ε of the form:

$$[\text{proMMP} - 2] = x_1/(1 + x_2\varepsilon + x_3\varepsilon^2) \qquad (3)$$

at both time points, but that less than 85% of this

Table 2 : Empirical regression analysis of strain effects[6]

Dependent variable	N [cyc]	Model	x1	x2	x3	PEV [%]
ProMMP-2 [ng/10K cells]	7,200	Eq. (3)	0.43	26.08	-122.8	81
	21,600	Eq. (3)	0.68	-7.15	25. 0	42
Network density [annuli/sq. mm]	7,200	Eq. (4)	0.40	-3.87		96
	21,600	Eq. (5)	-2.12	34	-84.0	96

is explained by dependence on strain amplitude alone. Further, we find that the density of annuli formed per mm^2 ρ_R is a strong function of strain amplitude at both time points:

$$\rho_R(4\text{hrs}) = x_1/(1 + x_2\varepsilon) \qquad (4)$$

$$\rho_R(12\text{hrs}) = exp(x_1 + x_2e - x_3\varepsilon^2) \qquad (5)$$

and that more than 95% of the variance in network density can be explained as a dependence on strain amplitude alone. Thus, it appears that cyclic strain indeed induces reorganization of EC monolayers in a manner that involves but is not explained wholly by increases in available MMP-2.

At 4 hrs (N = 7,200), the changes in secreted proMMP-2 levels and network formation are relatively well-correlated. That is, as proMMP-2 levels increase, ρ_R also increases. At 12 hrs (N = 21,600), the changes in secreted proMMP-2 levels appear to lead the organizational response of the cell population. That is, proMMP-2 levels peak and then decrease at ε = 0.12, whereas ρ_R peaks and then plateaus at ε = 0.18. We observed a similar trend for CECs at 24 hrs, with a peak of proMMP-2 levels and annulus density at ε = 0.20 and 0.27, respectively.

These data demonstrate only that there is a correlation between the amplitude and duration of cyclic strain on the secretion of proMMP-2 by ECs and the organization of EC populations, and that the strain amplitude sufficient to induce elevated protease secretion precedes that to induce cellular reorganization. However, there are several potential mechanisms which we can consider in light of previous studies, which may guide future hypotheses and investigations of the coupling between external strain communicated through the substrate to ECs and the corresponding enzyme secretion/organizational response of ECs *in vitro* and *in vivo*. Note that strain did not induce measurable activation of secreted proMMP-2, nor secretion of latent or active MMP-9 in either cell type. The lack of MMP-9 secretion is not entirely surprising; MMP-9 is expressed constitutively in other cell types involved in wound healing, but not in ECs [Mohan *et al.* (1998); Yan *et al.* (2000)]. This is in contrast to studies on cells which exert contractile forces on substrates such as fibroblasts, for which others have shown changes in the levels of both active and latent forms of these enzymes. Further, these findings provide an interesting comparison to those reported for human lung microvascular endothelial cells, which have been reported to show increasing levels of both pro- and active MMP-2 over a timescale of days for a fixed strain amplitude of ε = 0.18 and cyclic frequency ν = 0.5 Hz [Haseneen *et al.* (2003)]. (The authors did not report concurrent changes in cell population organization.) Although we observe increasing levels of proMMP-2 up to this strain amplitude within 12 hrs, we do not observe concurrent increases in active MMP-2 for these dermal MVECs.

It is reasonable to question the relevance of changes in the levels of the latent form of a protease, as this molecule cannot participate in ECM-degradation. However, it is clear that changes in proMMP-2 in fact represent changes

---

[6] PEV is a proportion explained by variance in strain amplitude, and is one measure of how well the model fits the data.

in the potential *availability of the reserve levels* of this key enzyme. Thus, it is plausible to construct a hypothesis from these results and Fig. 5 as follows: cyclic strain induces secretion of proMMP-2, thus increasing the reserves of this ECM-degradation enzyme. Beyond a critical strain amplitude, the reserves are depleted via conversion to active MMP-2, and cellular reorganization increases concurrently with increased ECM degradation.

Here, we were not able to determine how the total MMP-2 level (active and latent) changed as a function of time through enzyme-linked immunosorbent assay (ELISA) due to the insufficient sensitivity of this assay for the ng-scale enzyme levels quantified through zymography (despite up to 200-fold concentration of the supernatant). It is well-established that zymography is a more sensitive assay than ELISA, and uniquely measures the activity as distinct from the presence of an enzyme. Thus, it is unknown at present whether the total MMP-2 levels changed proportionally to the proMMP-2 levels. Upon activation, MMP-2 may be sequestered to the cell surface and pericellular ECM or degraded in the supernatant through autocatalysis. In both instances, zymographic analysis of the supernatant will not enable quantification of activated MMP-2. We were unsuccessful in detecting statistically significant levels of MMP-2 on or near the EC surface through immunocytochemistry via horseradish peroxidase-conjugated secondary antibody, but did confirm equivalent expression of vonWillenbrand factor (Factor VIII) by these cells before and after cyclic strain. Thus, future studies should consider sufficiently large supernatant volumes to enable significant concentration required for immunoassays, as well as alternative methods to quantify and distinguish presence of active MMP-2.

It is known that TIMP-2 can induce MMP-2 activity in a dose-dependent manner through a complex at the cell surface with MT1-MMP. Thus, we conducted an assay to quantify changes in TIMP-2 within the supernatant that may explain corresponding changes in active MMP-2 levels. This assay quantifies the percent-inhibition of collagenases by all TIMPs (not just TIMP-2) within the cell supernatant [Moses *et al.* (1990)]. Here, supernatant and collagenase are added to ^{14}C-labeled collagen-coated microtiter wells; collagenase activity degrades the radiolabeled collagen, and thus the intensity of the ^{14}C signal varies proportionally to the concentration of collagenase inhibitors such as TIMPs. If TIMP levels increased

concurrently with decreases in proMMP-2, it may be argued indirectly that active MMP-2 levels likely increased with increasing TIMP levels. We found that percent-inhibition and thus TIMP levels increased consistently when proMMP-2 levels decreased, but in a modest and statistically insignificant way with respect to experimental error of 10% (data not shown).

Certainly, the extent of strain-dependent cellular reorganization suggests that ECM-degradation and subsequent cell motility were enhanced by cyclic strain. Further, the correspondence between sharp decreases in proMMP-2 at strain levels concurrent with increases in the extent of annulus formation suggest, but do not prove, that increases in active MMP-2 facilitated the ECM-degradation required for significant reorganization of the EC monolayer. Future studies should consider evaluation of total MMP-2 mRNA levels as a function of external strain, as well as consideration of other MMPs which have been shown to be responsive to cyclic strain (at least at the mRNA level) in other cell types such as smooth muscle cells [Park *et al.* (1999)].

The relevance of this systematic *in vitro* study can be considered in the context of physiological and pathological states in which vascular endothelial cells are subjected to elevated strain and/or stress. Elevated mechanical stress may occur locally in the vascular wall via mechanical weakening resulting from trauma (overloading) or local proteolysis, or to stress concentrations resulting from increased vascular radius of curvature at branch points. This would suggest that enhancement of desirable vascular remodeling requires activation of existing MMPs rather than stimulation of additional MMPs. In addition, significant external compressive *and* tensile strain may be imposed by the growth of rigid, fluid-filled cysts or multicellular tumors [Gordon *et al.* (2003)]. Indeed, if external mechanical cues can induce ECM-degradation adjacent to existing vasculature *in vivo*, tumor angiogenesis may include a more complex interplay between MMP-secreting tumor cells and MMP-secreting vascular cells than is currently appreciated. Finally, although we did not design this study to compare the response of ECs as a function of mammalian origin or *in vivo* function, differences between these cell types may be due in part to these points. Future studies may consider how cell response to external strain depends on the basal mechanical state of such cells *in vivo*.

5 Conclusions

By systematically considering the extent to which cyclic strain affects the enzymatic response and organization of HMVEC and CEC populations, we conclude the following for both cell types:

- Cyclic mechanical strain induces a non-monotonic change in secreted proMMP-2 levels and the formation of multicellular networks of EC-dense struts resembling capillary tube-like structures observed under biochemical stimuli.

- The density of these networks increases with elapsed time/total cycles and strain amplitude, but the diameter of the EC-dense struts within the network do not increase significantly with time or strain for $\varepsilon > 0.05$ and slightly exceed that of capillary diameters.

- The strain amplitude required to maximize proMMP-2 secretion is less than that required to maximize network formation, suggesting that cells respond to cyclic strain by increasing the reserve of enzymes available for ECM degradation.

References

Apodaca, G.; Rutka, J. T.; Bouhana, K.; Berens, M. E.; Giblin, J. R.; Rosenblum, M. L.; McKerrow, J. H.; Banda, M. J. (1990): Expression of metalloproteinases and metalloproteinase inhibitors by fetal astrocytes and glioma cells. *Cancer Res.* vol. 50, pp. 128-133.

Davies, P. F.; Barbee, K. A.; Volin, M. V.; Robotewskyj, A.; Chen, J.; Joseph, L.; Griem, M. L.; Wernick, M. N.; Jacobs, E.; Polacek, D. C.; dePaola, N.; Barakat, A. I. (1997): Spatial relationships in early signaling events of flow-mediated endothelial mechanotransduction. *Annu Rev Physiol* vol. 59, pp. 527-549.

Davies, P. F.; Mundel, T.; Barbee, K. A. (1995): A mechanism for heterogeneous endothelial responses to flow in vivo and in vitro. *J Biomech* vol. 28, pp. 1553-1560.

Drenckhahn, D.; Ness, W. (1997): In: Vascular Endothelium: Physiology, Pathology and Therapeutic Opportunities, eds. C.J. Schwartz and G.V.R. Born, Stuttgart: Schattauer, pp. 1-25.

Fang, J.; Shing, Y.; Wiederschain, D.; Yan, L.; Butterfield, C.; Jackson, G.; Harper, J.; Tamvakopoulos, G.; Moses, M. A. (2000): *Proc. Nat. Acad. Sci.* vol. 97, pp. 3884-3889.

Folkman, J.; Haudenschild, C. (1980): Angiogenesis in vitro. *Nature* vol. 288, pp. 551-556.

Gordon, V.; Valentine, M.; Gardel, M.; Andor-Ardo, D.; Dennison, S.; Bogdanov, A.; Weitz, D.; Deisboeck, T. (2003): Measuring the mechanical stress induced by an expanding multicellular tumor system: a case study. *Exp Cell Res* vol. 289, pp. 58-66.

Hanahan, D.; Folkman, J. (1996): Patterns and emerging mechanisms of the angiogenic switch during tumorigenesis. *Cell* vol. 86, pp. 353-364.

Haseneen, N.; Vaday, G. G.; Zucker, S.; Foda, H. G. (2003): Mechanical stretch induces MMP-2 release and activation in lung endothelium: role of EMMPRIN. *Am. J. of Lung, Cell. Mol. Phys*, vol. 284, pp. L541 - 547.

Hsiai, T. K.; Cho, S. K.; Honda, H. M.; Hama, S.; Navab, M.; Demer, L. L.; Ho, C. M. (2002): Endothelial cell dynamics under pulsating flows: significance of high versus low shear stress slew rates (d(tau)/dt). *Ann Biomed Eng* vol. 30, pp. 646-656.

Ingber, D. E. (2002): Mechanical signaling and the cellular response to extracellular matrix in angiogenesis and cardiovascular physiology. *Circ Res* vol. 91, pp. 877-887.

Kheradmand, F.; Werner, E.; Tremble, P.; Symons, M.; Werb, Z. (1998): Role of Rac1 and oxygen radicals in collagenase-1 expression induced by cell shape change. *Science* vol. 280, pp. 898-902.

Kubota, Y.; Kleinman, H. K.; Martin, G. R.; Lawley, T. J. (1988): Role of laminin and basement membrane in the morphological differentiation of human endothelial cells into capillary-like structures. *J Cell Biol* vol. 107, pp. 1589-1598.

Lee, A.; Graham, D.; Dela Cruz, S.; Ratcliffe, A.; Karlon, W. (2002): Fluid shear stress-induced alignment of cultured vascular smooth muscle cells. *J Biomech Eng.* vol. 124, pp. 37-43.

Liu, Y.; Chen, B. P.; Lu, M.; Zhu, Y.; Stemerman, M.

B.; Chien, S.; Shyy, J. Y. (2002): Shear stress activation of SREBP1 in endothelial cells is mediated by integrins. *Arterioscler Thromb Vasc Biol* vol. 22, pp. 76-81.

Lohi, J.; Lehti, K.; Maltanen, H.; Parks, W.; Keski-Oja, J. (2000): Structural analysis and promoter characterization of the human membrane-type matrix metalloproteinase-1 (MT1-MMP) gene. *Gene* vol. 242, pp. 75-86.

Maciag, T.; Kadish, J.; Wilkins, L.; Stemerman, M.; Weinstein, R. (1982). Organizational behavior of human umbilical vein endothelial cells. *J Cell Biol* vol. 94, pp. 511-520.

Mohan, R.; Rinehart, W.; Bargangna-Mohan, P.; Fini, M. (1998): Gelatinase B/lacZ transgenic mice, a model for mapping gelatinase B expression during developmental and injury-related tissue remodeling. *J. Biol. Chem.* vol. 273, pp. 25903-25914.

Moses, M. A. (1997): The regulation of neovascularixation by matrix metalloproteinases. *Nat. Med.* vol. 5, pp. 434-438.

Moses, M. A.; Sudhalter, J.; Langer, R. (1990): Identification of an inhibitor of neovascularization from cartilage. *Science* vol. 248, pp. 1408-1410.

Nagase, H.; Woessner, J. J. (1999): Matrix metalloproteinases. *J. Biol. Chem.* vol. 274, pp. 21491-21494.

Nakano, A.; Tani, E.; Miyazaki, K.; Yamamoto, Y.; Furuyuma, J. I. (1995): Matrix metalloproteinases and inhibitors of metalloproteinases in human gliomas. *J. Neurosurg.* vol. 83, pp. 298-305.

Park, J. M.; Adam, R. M.; Peters, C. A.; Guthrie, P. D.; Sun, Z.; Klagsbrun, M.; Freeman, M. R. (1999): AP-1 mediates stretch-induced expression of HB-EGF in bladder smooth muscle cells. *American Phy. Society* vol. 99, pp. 294-301.

Prajapati, R. T.; Chavally-Mis, B.; Herbage, D.; Eastwood, M.; Brown, R. A. (2000a): Mechanical loading regulates protease production by fibroblasts in three-dimensional collagen substrates. *Wound Rep. Reg.* 8, pp. 226-237.

Prajapati, R. T.; Eastwood, M.; Brown, R. A. (2000b): Duration and orientation of mechanical loads determine fibroblast cyto-mechanical activation: Monitored by protease release. *Wound Rep. Reg.* vol. 8, pp. 238-246.

Resnick, N.; Yahav, H.; Shay-Salit, A.; Shushy, M.; Schubert, S.; Zilberman, L. C.; Wofovitz, E. (2003): Fluid shear stress and the vascular endothelium: for better and for worse. *Prog Biophys Mol Biol* vol. 81, pp. 177-199.

Shyy, J. Y.; Chien, S. (2002): Role of integrins in endothelial mechanosensing of shear stress. *Circ Res* vol. 91, pp. 769-775.

Sternlicht, M.; Bergers, G. (2000): Matrix metalloproteinases as emerging targets in anti-cancer therapy: status and prospects. *Emerging Ther. Targets* vol. 4, pp. 609-633.

Strongin, A.; Collier, I.; Bannikov, G.; Marmer, B.; Grant, G.; Goldberg, G. (1995): Mechanism of cell surface activation of 72-kDa type IV collagenase. Isolation of the activated form of the membrane metalloprotease. *J. Biol. Chem.* vol. 270, pp. 5331-5338.

Weinbaum, S.; Zhang, X.; Han, Y.; Vink, H.; Cowin, S. C. (2003): Mechanotransduction and flow across the endothelial glycocalyx. *Proceedings of the National Academy of Science U.S.A.* vol. 100, pp. 7988-7995.

West, J. B.; Mathieu-Costello, O. (1995): *Circulation* vol. 92, pp. 622-631.

Yan, L.; Moses, M. A.; Huang, S.; Ingber, D. E. (2000): Adhesion-dependent control of matrix metalloproteinase-2 activation in human capillary endothelial cells. *J Cell Sci* vol. 113, pp. 3979-3987.